ORIGINAL ARTICLE

Preparation and physical properties of $(PVA)_{0.7}(NaBr)_{0.3}(H_3PO_4)_{x}$M solid acid membrane for phosphoric acid – Fuel cells

F. Ahmad [a],*, E. Sheha [b]

[a] *Physics Department, Faculty of Science, Al-Azhar University, Girls Branch, Cairo, Egypt*
[b] *Physics Department, Faculty of Science, Benha University, Benha, Egypt*

Abstract A solid acid membranes based on poly (vinyl alcohol) (PVA), sodium bromide (NaBr) and phosphoric acid (H_3PO_4) were prepared by a solution casting method. The morphological, IR, electrical and optical properties of the $(PVA)_{0.7}(NaBr)_{0.3}(H_3PO_4)_{x}$M solid acid membranes where $x = 0.00, 0.85, 1.7, 3.4, 5.1$ M were investigated. The variation of film morphology was examined by scanning electron microscopy (SEM) studies. FTIR spectroscopy has been used to characterize the structure of polymer and confirms the complexation of phosphoric acid with host polymeric matrix. The temperature dependent nature of ionic conductivity and the impedance of the polymer electrolytes were determined along with the associated activation energy. The ionic conductivity at room temperature was found to be strongly depends on the H_3PO_4 concentration which it has been achieved to be of the order 4.3×10^{-3} S/cm at ambient temperature. Optical measurements showed a decrease in optical band gap and an increase in band tail width with the increase of phosphoric acid. The data shows that the $(PVA)_{0.7}(NaBr)_{0.3}(H_3PO_4)_{x}$M solid acid membrane is promising for intermediate temperature phosphoric acid fuel cell applications.

Introduction

The research activities in the solid proton conductive polymer electrolytes dramatically increased due to their potential application in industrial chemical energy convention devices such as proton exchange membrane fuel cells (PEMFC) [1]. Especially research trend has been focused on the development of anhydrous or low humidity polymer electrolytes to maintain adequate proton conductivity at higher temperatures. Since, the operation of fuel cells at higher temperatures, i.e., in excess of 100 °C, provides additional advantages such as, improvement of CO tolerance of platinum catalyst, improve mass transportation, increase reaction kinetics and simplify the water management and gas humidification [2,3].

Humidified perfluorosulfonic acid membranes such as Nafion have been widely investigated in fuel cell applications

* Corresponding author. Tel.: +20 1113022588; fax: +20 22629356.
E-mail address: Fatma.Ahmad@ymail.com (F. Ahmad).

due to its high proton conductivity below 100 °C. Despite their high thermal and chemical stability, these membrane materials have some disadvantages including complex external humidification, high material cost and high methanol crossover where these have slowed down their widespread industrial application [4,5].

In order to overcome those limitations, a number of studies have been performed to produce novel polymer-based materials that can transport protons under anhydrous conditions. In this context, phosphoric acid based systems are widely studied for that purpose since pure H_3PO_4 itself is a good proton conductor because of its extensive self-ionization and low acid dissociation constant pKa. PVA was used as host polymers that keep phosphoric acid in their matrix and proton transport is mainly provided by phosphoric acid units via structure diffusion where the transference number of proton is close to unity [6,7].

Although several homogeneous polymer electrolytes were reported in earlier studies [8–11], phosphoric acid doped polybenzimidazole (PBI), showed better physicochemical properties and promising fuel cell performance [12–15].

Although high proton conductivity can only be achieved at higher acid compositions, dopant exclusion is an important drawback during prolonged usage in fuel cells. Therefore, our work has been driven by a desire to develop a radically new, alternative proton-conducting electrolyte (or membrane) that is based on compounds whose chemistry and properties are intermediate between those of a normal acid, such as H_3PO_4, and a normal salt, such as NaBr and not a hydrated polymer (solid acid). Thus, membranes will be developed, in which a solid acid is embedded in PVA matrix, with the polymer providing mechanical support and enhancing chemical stability.

In this study, an attempt has been made to prepare the polymer electrolytes based on PVA–NaBr complexed with H_3PO_4 at different concentrations expect to use it in fuel cell application. Another approach to the development of proton-conducting membranes is to combine the functions of the Hydroquinone (HQ) and the proton solvent in a single molecule. Such molecules must be amphoteric in the sense that they behave as both a proton donor (acid) and proton acceptor (base), and they must form dynamical hydrogen bonds. Also HQ plays a major role as a reducing agent for bromine and improving the chemical stability of the matrix [16].

The current work is aimed to improve the electrical properties of $(PVA)_{0.7}(NaBr)_{0.3}$ through doping in different proportions of phosphoric acid. In similar study, the results of addition of HQ to $(PVA)_{0.7}$, lithium bromide $(LiBr)_{0.3}$, sulfuric acid $(H_2SO_4)_{2.9}$ and 2%(w/v) ethylene carbonate, revealed that, the thermal stability and electrical conductivity of the samples improve on increasing the HQ doping. The film doped with 4 wt% HQ exhibits maximum conductivity was found to be 1.75×10^{-3} S/cm at room temperature [16].

In the present work, 0.4% (w/v) HQ and 2% (w/v) ethylene carbonate which used as plasticizer were added to $(PVA)_{0.7}$ $(NaBr)_{0.3}(H_3PO_4)_{xM}$ membrane to improve the electrical and structural properties. However, the addition of NaBr to pure PVA enhances the electrical properties where the conductivity increases from 10^{-9} to 10^{-6} S/cm with addition NaBr up to 30% ratio [17]. The synthesis of polymers $(PVA)_{0.7}$ $(NaBr)_{0.3}(H_3PO_4)_{xM}$ and molecular interactions within the membranes, surface morphologies, IR and optical properties of the membranes were investigated. Effects of H_3PO_4 contents on proton conductivity of final product were discussed.

Experimental

Dilute solution of 7% (w/v) PVA with molecular weight ∼1800 (QualiKems chemical India), 3% (w/v) NaBr (Sigma), 0.4% (w/v) hydroquinone and 2% (w/v) ethylene carbonate in H_2O and 1 cm^3 of H_3PO_4 $_{xM}$ (GPR-ADWIC) in different molar ratios (where x = 0.00, 0.85, 1.7, 3.4, 5.1 M) were prepared in stoppered conical flask. The resulting solutions were finally stirred for 2 h. It was then cast in petri-glass dishes. Films were dried for four weeks to evaporate water content. The final product was vacuum dried for 6 h. The surface morphology of membranes was investigated by scanning electron microscopy (SEM, JOEL-JSM Model 5600).

Infrared spectrum is a finger print which gives sufficient information about the structure of a compound. In order to clarify the nature of the interactions and complexation between $(PVA)_{0.7}(NaBr)_{0.3}(H_3PO_4)_{xM}$, IR spectra of PVA complexes of different molar ratios in film form have been recorded using FTIR Jasco 6300 a spectrometer for wavenumber range between 400 and 2000 cm^{-1}.

Optical measurements were done by using UV–visible recording spectrophotometer (UV–visible JenWay 6405), the transmission $T\%$ were measured in the spectral range 190–1100 nm at room temperature.

Electrical measurements were performed on PM 6304 programmable automatic RCL (Philips) meter in the frequency ranging from 60 Hz to 100 kHz at different temperatures. Samples of diameter 0.5 cm and thickness ∼0.1 mm were sandwiched between two brass electrodes of a spring-loaded sample holder. The whole assembly was placed in an oven monitored by a temperature controller. The rate of heating was adjusted to be 2 K/min.

Results and discussion

Morphological studies

The morphology of the polymer can be studied using the SEM. This technique provides further information about the structural modifications of the polymer under consideration with dopant. Fig. 1 shows scanning electron microscopy images of the surface morphology of three selected polymer electrolyte membranes hybridized with H_3PO_4. Very distinguishable changes can be observed from pure (0.00 M), intermediate (0.85 M) and high concentration of H_3PO_4 (3.4 M). The 0.00 M membrane displays a surface with long regular braids of PVA, Fig. 1a. In contrast, the 0.85 and 3.4 M doped membranes show no phase separation occurred during solvent evaporation, hence homogeneous films formed. This result indicates to interaction between of phosphoric acid and polymer blend, hence enhancement of amorphous nature [18,19]. Also the addition of H_3PO_4 shows a large number of voids, Fig. 1b and c. An open void structure of the polymer electrolyte matrix is essential for ionic conductivity. This type of open porus structure provides enough channels for the migration of ions, account for better ionic conductivity.

FTIR spectroscopy

FT-IR spectroscopy is important in the investigation of polymer structure, since it provides information about the
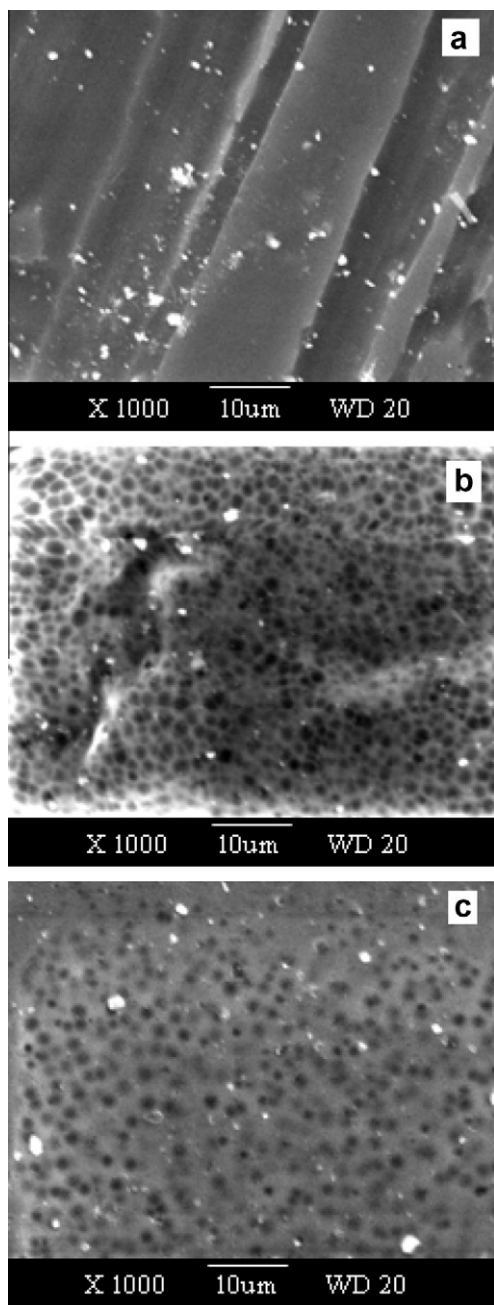
Fig. 1 The SEM for $(PVA)_{0.7}(NaBr)_{0.3}(H_3PO_4)_{xM}$ with 0.00 M (a), 0.85 M (b), and 3.4 M (c).

complexation and interactions between the various constituents in the polymer electrolyte. IR Spectra of pure PVA and its complexes with H_3PO_4 in different content ($x = 0.00$, 0.85, 1.7, 3.4 M) is shown in Fig. 2. The stretching vibrational bands of C=O appeared at ~1775 and 1640 cm^{-1} which attributed to the carbonyl functional groups due to the residual acetate groups remaining after the manufacture of PVA from hydrolysis of polyvinyl acetate or oxidation during manufacturing and processing. The bands locate less than 1500 cm^{-1} assignment to PVA polymer formation [20–23]. It is found that C—O stretching causes a spectral band at ~1383 cm^{-1} and intensity of this band decreases. This may occur due to

decreasing number of C—O groups in the membrane [24]. The absorption band at ~1091 cm^{-1} was attributed to the C—O stretching vibration of the hydroxy group. The intensity of the hydroxy C—O band was a measure of the degree of crystallinity of PVA [23–25]. Fig. 2 (inset) represents composition dependence of the relative area under band at 1091 cm^{-1} which was determined from spectra deconvolution into Gaussian components to give the best fit using non-linear least squares fitting method. It is clear that the addition of phosphoric acid leads to decrease the relative area. Thus, this result supported the suggestion that the degree of crystallinity of membranes decrease [26], which was consistent with the SEM results. A new absorption peak at ~990 cm^{-1} is observed in phosphoric acid doped membranes due to vibration of —CH$_2$—O—P—O. IR spectra results prove that the complexation of PVA with H_3PO_4 [24].

Conductivity studies

The conductivities of the polymer complexes were calculated from the bulk resistance obtained by the intercepts of the typical impedance curves (Cole–Cole) for various films concentration. The real and imaginary parts were taken along the x- and y-axes, respectively. Intercept of the curve on the real axis gives the bulk resistance (R_b) of the sample. The bulk conductivities σ_b were calculated using the relation [27]:

$$\sigma_b = \frac{l}{R_b A} \tag{1}$$

where l is the thickness, R_b is bulk resistance, and A is the contact area of the electrolyte film during the experiment.

The bulk conductivity as a function of H_3PO_4 concentration at room temperature is shown in Fig. 3 (inset). We can notice a pronounced effect on the conductivity as σ follows an increasing trend. The conductivity of pure $(PVA)_{0.7}(NaBr)_{0.3}$ is $\sim 10^{-6}$ S/cm [17] and it increases up to 4.3×10^{-3} S/cm on complexing the $(PVA)_{0.7}(NaBr)_{0.3}$ with H_3PO_4 concentration. Enhancement in the conductivity of PVA complexes may be due to increase number of mobile charge H$^+$ ions from H_3PO_4. As well as the presence of H_3PO_4 in the complexes decreases the viscosity of the sample which in turn makes the polymeric chain flexible and consequently easy bond rotation reinforce the transportation of ions in the complexes [24]. Generally, ionic conductivity of electrolyte depends on the charge carrier concentration, n, and carrier mobility, μ, as described by the relation:

$$\sigma = nq\mu \tag{2}$$

where n, q and μ representing the charge carrier concentration, charge of mobile carrier and the mobility, respectively.

Temperature dependence of conductivity $\sigma(\omega)$ for all samples is shown in Fig. 4. It was observed that as the temperature increases, the conductivity also increases for all of the films where up to 1.8×10^{-2} S/cm for $x = 5.1$ M at 373 K. This behavior is in agreement with the theory established by Armand et al., this is rationalized by considering the free volume model [27]. When the temperature increases, the vibrational energy of a segment is sufficient to push against the hydrostatic pressure imposed by its neighboring atoms and creates a small amount of space surrounding its own volume in which vibrational motion can occur [28]. Therefore, the free volume
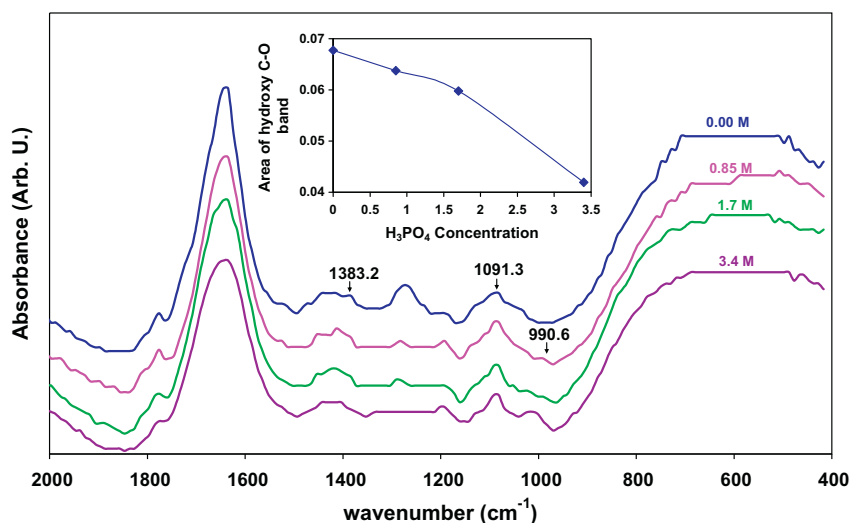
Fig. 2 FTIR spectra for films of $(PVA)_{0.7}(NaBr)_{0.3}(H_3PO_4)_{xM}$ where $x = 0.00$, 0.85, 1.7, 3.4 M. The inset represents composition dependence of the relative area under the hydroxy C—O band.
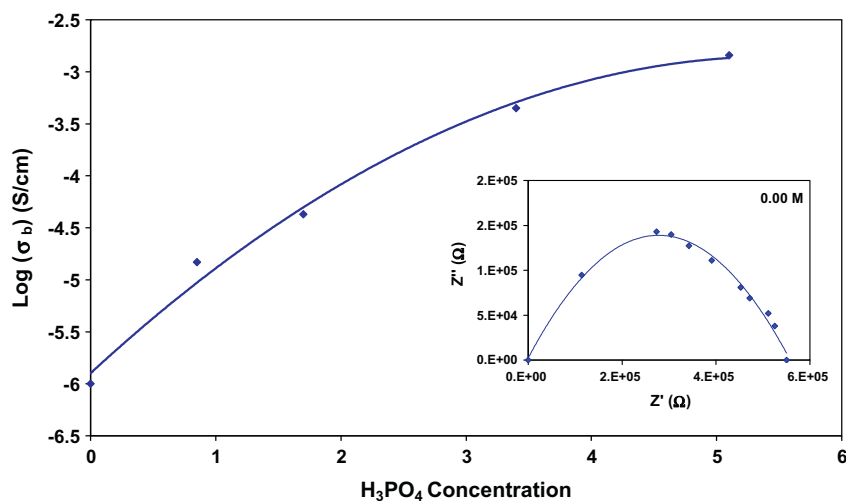

Fig. 3 Influence of H_3PO_4 content on bulk conductivity of $(PVA)_{0.7}(NaBr)_{0.3}(H_3PO_4)_{xM}$ solid acid membrane at room temperature. The inset represents the cole–cole diagram for 0.00 M sample.

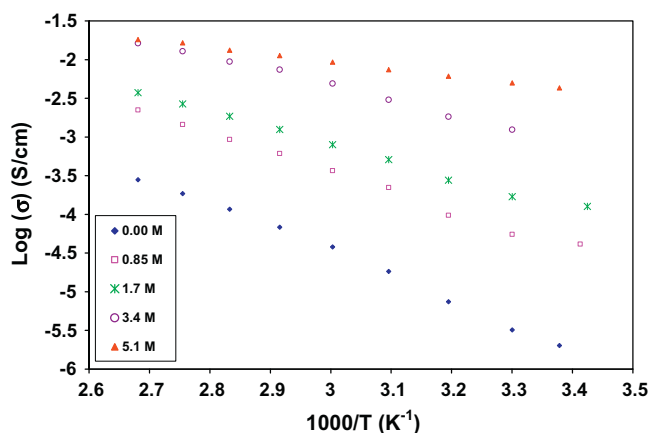**Fig. 4** The temperature dependence of conductivity for $(PVA)_{0.7}(NaBr)_{0.3}(H_3PO_4)_{xM}$ solid acid membrane at 1 kHz.

around the polymer chain causes the mobility of the ions to increase and, due to the segmental motion of the polymer, causes the conductivity to increase. Hence, increasing the temperature causes the conductivity to increase due to the increased free volume and their respective ionic and segmental mobility. The conductivity–temperature relationship of this system can be characterized as Arrhenius behavior, suggesting that conductivity is thermally assisted. The activation energy (E_a) of the membrane can be calculated using Arrhenius equation [29]:

$$\sigma = \sigma_o \exp\left(\frac{-E_a}{k_B T}\right) \tag{3}$$

where σ_o is the pre exponential factor, k_B the Boltzmann constant and T is the temperature in Kelvin. Table 1 shows the relationship between E_a and phosphoric acid concentration. The results show an inverse relationship between E_a and phosphoric acid concentration; the highest concentration

Table 1 The activation energy, conductivity at fixed frequencies and optical parameters values of $(PVA)_{0.7}(NaBr)_{0.3}(H_3PO_4)_{xM}$ films.

H_3PO_4 concentration (M)	Activation energy (eV)	Conductivity at room temperature (S/cm)			Optical parameters (eV)	
		100 Hz	1 kHz	100 kHz	Band gap energy	Band tail width
0.00	0.63	1.74E−06	2.02E−06	6.23E−06	3.57	0.34
0.85	0.52	3.90E−05	4.13E−05	4.44E−05	3.52	0.49
1.7	0.44	1.08E−04	1.27E−04	1.45E−04	3.47	0.56
3.4	0.37	9.84E−04	1.24E−03	1.82E−03	3.44	0.62
5.1	0.19	3.26E−03	4.30E−03	6.43E−03	3.36	0.68

membranes yields the lowest E_a. Normally the highest conductivity sample will give the lowest E_a. It is noteworthy that the polymer electrolytes with low values of activation energies are desirable for practical applications.

Normally, there are two different transport mechanisms that contribute to the proton conductivity in phosphoric acid-doped polymer electrolytes. The first is the structural diffusion (Grotthuss mechanism) in which the conductivity is mainly controlled by proton transport through phosphate ions, i.e. $H_4PO_4^+, H_2PO_4^-$ (Grotthuss proton transport). The second is the vehicle mechanism where the protons travel through the material on a neutral or charged "vehicle". Several studies were reported about the contribution of these mechanisms on the proton conductivity of pure phosphoric acid and it was indicated that the former is much more predominant and the conduction mechanism is mainly controlled by the structural diffusion rather than vehicle mechanism. It is clear that, there is significant proton conductivity of phosphoric acid doped samples may be attributed to the major part of the proton transport is provided over H_3PO_4.

Table 1 shows the room temperature conductivity at 100 Hz, 1 kHz and 100 kHz for all $(PVA)_{0.7}(NaBr)_{0.3}(H_3PO_4)_{xM}$ membrane. The frequency dependent of the conductivity $\sigma(\omega)$ were measured using the following equation [7]:

$$\sigma(\omega) = \varepsilon''(\omega)\omega\varepsilon_o \qquad (4)$$

where ε'' the imaginary part of dielectric constant, ω is the angular frequency and ε_o is permittivity of free space. The frequency response of the conductivity is interpreted in terms of jump relaxation model [28], where the conduction is due to translation and localized hopping. According to jump relaxation model, at very low frequencies an ion can jumps from one site to its neighboring vacant site successfully contributing to the dc conductivity. At higher frequencies, the probability for the ion to go back again to its initial site increases due to the short time periods available. The overall behavior of conductivity follows universal dynamic process, which has been widely observed in disordered materials like ion conducting polymers and glasses [30].

Dielectric properties

The study of dielectric relaxation in solid polymer electrolytes is a powerful approach for obtaining information about the characteristics of ionic and molecular interactions. The dielectric parameters associated with relaxation processes are of particular significance in ion conducting polymers where the dielectric constant plays a fundamental role which shows the ability of a polymer material to dissolve salts. The dielectric constant was used as an indicator to show that the increase

in conductivity is mainly due to an increase in the number density of mobile ions [31]. The frequency-dependent conductivity and dielectric relaxation are both sensitive to the motion of charged species and dipoles of the polymer electrolytes.

The complex dielectric constant of a system ε^* is defined by:

$$\varepsilon^* = \varepsilon' - i\varepsilon'' \qquad (5)$$

Real part of dielectric constant ε' of the material is expressed as:

$$\varepsilon' = Cl/\varepsilon_o A \qquad (6)$$

where C is parallel capacitance. The variation of the real part of the dielectric constant ε' as a function of frequency for all the samples is shown in Fig. 5a. The observed variation in ε'
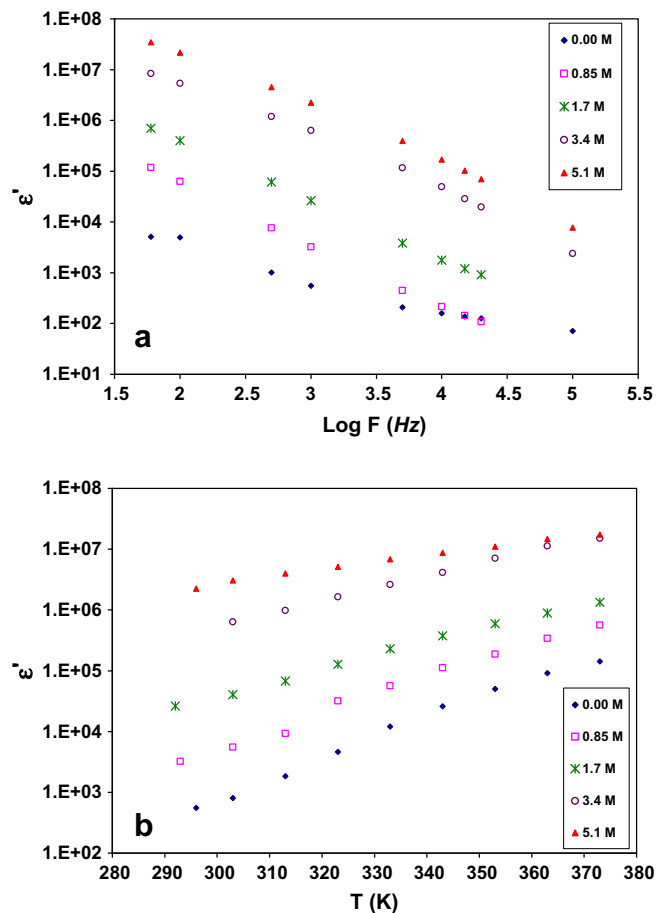

Fig. 5 Real part of dielectric constant as a function of (a) frequency at room temperature, and (b) temperature at 1 kHz.

with frequency could be attributed to the formation of a space charge region at the electrode and electrolyte interface, which is known as the non-Debye type of behavior where the space charge regions with respect to the frequency is explained in terms of ion diffusion [32]. The material electrode interface polarization of the composites masks the other relaxation processes at low frequencies [33]. On the other hand, with increasing frequency there is no time for charge build-up at the interface because of the increasing rate of reversal of the electric field. Therefore, the polarization due to charge accumulation decreases which leads to the decreases in the value of ε' [31]. The variation of the real ε' of the dielectric constant as a function of temperature for all the samples are shown in Fig. 5b. The observed increase in ε' with temperature could be attributed to decrease in the viscosity of the polymeric material. This leads to an increment in the degree of dipole orientation of polar dielectric material and hence dielectric constant increases [34]. Dipolar molecules should be able to orient from one equilibrium position to another relatively easily, and contribute to absorption [33].

Optical properties

The optical properties of polymers can be suitably modified by the addition of dopants depending on their reactivity with the host matrix [35]. The optical absorption spectrum is an important tool to obtain optical band gap energy of crystalline and amorphous materials. The fundamental absorption, which corresponds to the electron excitation from the valance band to the conduction band, can be used to determine the nature and value of the optical band gap. The relation between the absorption coefficient (α) and the incident photon energy ($h\nu$) can be written as [36,37]:

$$\alpha h\nu = C(h\nu - E_o)^m \tag{7}$$

where C is a constant, E_o is the optical band gap of the material and the exponent m depends on the type of transition. m is an index which can be assumed to have values of 1/2, 3/2, 2 and 3, depending on the nature of the electronic transition responsible for absorption, m is equal to 1/2 for allowed direct transitions, 3/2 for direct forbidden transitions, 2 for allowed indirect transitions and 3 for forbidden indirect transitions. The indirect band gaps of films E_o can be obtained from Eq. (7) by extrapolating linear portion of $(\alpha h\nu)^{1/2}$ to zero absorption in the $(\alpha h\nu)^{1/2}$ vs. $h\nu$ plot as shown in Fig. 6. The lack of crystalline long-range order in amorphous materials is associated with a tailing of the density of states into the normally forbidden energy band. The absorption coefficient is given by El-Khodary [37]:

$$\alpha(\omega) = \alpha_o \exp(h\nu/E_t) \tag{8}$$

where α_o is a constant and E_t is the band tail width. The values of E_t are calculated from the slopes of the straight lines of $\ln\alpha$ as a function of photon energy ($h\nu$) according to Eq. (8). Table 1 shows the optical gap and the band tail composition dependence, it is clear that both the optical gap and the band tail are behaving oppositely. The addition of H_3PO_4 causes a decrease in E_o which may be explained on the basis of the incorporation of amounts of dopant forms charge transfer complexes (CTCs) in the host lattice, which enhance the lower energy transitions leading to the observed change in optical band gap. These
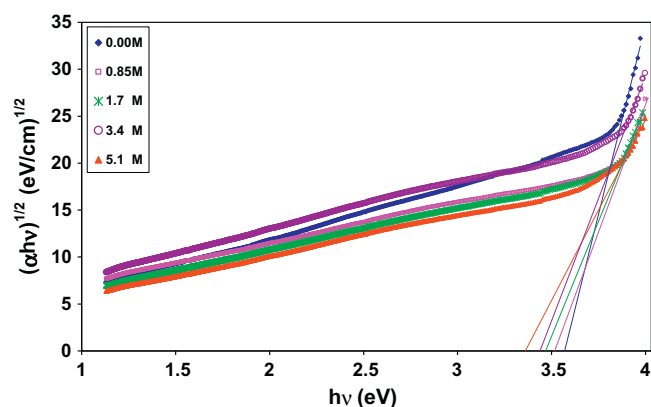

Fig. 6 The $(\alpha h\nu)^{1/2}$ vs. photon energy ($h\nu$) plots of $(PVA)_{0.7}$ $(NaBr)_{0.3}(H_3PO_4)_{xM}$ films.

CTCs increase the electrical conductivity by providing additional charges in the lattice and hence, a decrease of activation energy [38,39].

Conclusion

The novel polymer membrane, based on $(PVA)_{0.7}(NaBr)_{0.3}$ $(H_3PO_4)_{xM}$, was obtained using a solution casting method. SEM and IR spectra prove that the complexation of PVA with H_3PO_4 and degree of crystallinity of membranes decrease with increase H_3PO_4 content. The addition of H_3PO_4 to the PVA–NaBr polymer electrolytes has proved to be a convenient method to increase the ionic conductivities of the membranes to 4.3×10^{-3} S/cm at ambient temperature. The increase of temperature increases the conductivity where up to 1.8×10^{-2} S/cm for $x = 5.1$ M at 373 K. The increase of degree of amorphousity in the polymeric material increases ε' values. The decrease in optical band gap and increase in band tail width can be correlated to the formation of the charge transfer complexes within the polymer network on dispersing H_3PO_4 in it. From a practical point of view, the $(PVA)_{0.7}(NaBr)_{0.3}(H_3PO_4)_{xM}$ solid acid membrane is a potential candidate for phosphoric acid fuel cell application.

References

[1] Prajapati GK, Gupta PN. Comparative study of the electrical and dielectric properties of PVA–PEG–Al$_2$O$_3$–MI (M = Na, K, Ag) complex polymer electrolytes. Physica B 2011;406(15–16):3108–13.
[2] Mehta V, Cooper JS. Review and analysis of PEM fuel cell design and manufacturing. J Power Source 2003;114(1):32–53.
[3] Shen Y, Xi J, Qiu X, Zhu W. A new proton conducting membrane based on copolymer of methyl methacrylate and 2-acrylamido-2-methyl-1-propanesulfonic acid for direct methanol fuel cells. Electrochim Acta 2007;52(24):6956–61.
[4] Bae B, Kim D. Sulfonated polystyrene grafted polypropylene composite electrolyte membranes for direct methanol fuel cells. J Membrane Sci 2003;220(1–2):75–87.
[5] Fu Y, Manthiram A, Guiver MD. Blend membranes based on sulfonated poly(ether ether ketone) and polysulfone bearing benzimidazole side groups for proton exchange membrane fuel cells. Electrochem Commun 2006;8(8):1386–90.

[6] Dippel Th, Kreuer KD, Lassègues JC, Rodriguez D. Proton conductivity in fused phosphoric acid; a $^1H/^{31}P$ PFG-NMR and QNS study. Solid State Ionics 1993;61(1–3):41–6.

[7] Çelik SÜ, Aslan A, Bozkurt A. Phosphoric acid-doped poly(1-vinyl-1,2,4-triazole) as water-free proton conducting polymer electrolytes. Solid State Ionics 2008;179(19–20):683–8.

[8] Donoso P, Gorecki W, Berthier C, Defendini F, Poinsignon C, Armand MB. NMR, conductivity and neutron scattering investigation of ionic dynamics in the anhydrous polymer protonic conductor $PEO(H_3PO_4)_x$. Solid State Ionics 1988;28–30(2):969–74.

[9] Aslan A, Çelik SÜ, Bozkurt A. Proton-conducting properties of the membranes based on poly(vinyl phosphonic acid) grafted poly(glycidyl methacrylate). Solid State Ionics 2009;180(23–35):1240–5.

[10] Daniel MF, Desbat B, Cruege F, Trinquet O, Lassegues JC. Solid state protonic conductors: poly(ethylene imine) sulfates and phosphates. Solid State Ionics 1988;28–30(1):637–41.

[11] Tanaka R, Yamamoto H, Shono A, Kubo K, Sakurai M. Proton conducting behavior in non-crosslinked and crosslinked polyethylenimine with excess phosphoric acid. Electrochim Acta 2000;45(8–9):1385–9.

[12] Samms SR, Wasmus S, Savinell RF. Thermal stability of proton conducting acid doped polybenzimidazole in simulated fuel cell environments. J Electrochem Soc 1996;143(4):1225–32.

[13] Li Q, He R, Gao J-A, Jensen JO, Bjerrum NJ. The CO poisoning effect in PEMFCs operational at temperatures up to 200 °C. J Electrochem Soc 2003;150(12):A1599–605.

[14] Pu H, Meyer WH, Wegner G. Proton transport in polybenzimidazole blended with H_3PO_4 or H_2SO_4. J Polym Sci B Polym Phys 2002;40(7):663–9.

[15] Zhai Y, Zhang H, Zhang Y, Xing D. A novel H_3PO_4/Nafion–PBI composite membrane for enhanced durability of high temperature PEM fuel cells. J Power Source 2007;169(2):259–64.

[16] Samy B, Sheha E. Impact of hydroquinone on thermal and electrical properties of plasticized [poly(vinyl alcohol)]$_{0.7}(LiBr)_{0.3}(H_2SO_4)_{2.9}$ mol L^{-1} solid acid membrane. Polym Int 2011;60(7):1142–8.

[17] Sheha E, El-Mansy MK. A high voltage magnesium battery based on H_2SO_4-doped $(PVA)_{0.7}(NaBr)_{0.3}$ solid polymer electrolyte. J Power Source 2008;185(2):1509–13.

[18] Pu H-T, Qiao L, Liu Q-Z, Yang Z-L. A new anhydrous proton conducting material based on phosphoric acid doped polyimide. Eur Polym J 2005;41(10):2505–10.

[19] Aslan A, Çelik SÜ, Şen Ü, Hasera R, Bozkurt A. Intrinsically proton-conducting poly (1-vinyl-1,2,4-triazole)/triflic acid blends. Electrochim Acta 2009;54(11):2957–61.

[20] Amaral FA, Dalmolin C, Canobre ShC, Bocchi N, Rocha-Filho RC, Biaggio SR. Electrochemical and physical properties of poly(acrylonitrile)/poly(vinyl acetate)-based gel electrolytes for lithium ion batteries. J Power Source 2007;164(1):379–85.

[21] Bhargav PB, Mohan VM, Sharma AK, Rao VVRN. Investigations on electrical properties of (PVA:NaF) polymer electrolytes for electrochemical cell applications. Curr Appl Phys 2009;9(1):165–71.

[22] Mansur HS, Sadahira CM, Souza AN, Mansur AAP. FTIR spectroscopy characterization of poly (vinyl alcohol) hydrogel with different hydrolysis degree and chemically crosslinked with glutaraldehyde. Mater Sci Eng C 2008;28(4):539–48.

[23] Gupta PN, Singh KP. Characterization of H_3PO_4 based PVA complex system. Solid State Ionics 1996;86–88(1):319–23.

[24] Wang H, Fang P, Chen Z, Wang S. Synthesis and characterization of CdS/PVA nanocomposite films. Appl Surf Sci 2007;253(1):8495–9.

[25] Ali ZI, Ali FA, Hosam AM. Effect of electron beam irradiation on the structural properties of PVA/V_2O_5 xerogel. Spectrochim Acta A Mol Biomol Spectrosc 2009;72(4):868–75.

[26] Hassan MA, Gouda ME, Sheha E. Investigations on the electrical and structural properties of PVA doped with $(NH_4)_2SO_4$. J Appl Polym Sci 2010;116(2):1213–7.

[27] Varishetty MM, Qiu W, Gao Y, Chen W. Structure, electrical and optical properties of $(PVA/LiAsF_6)$ polymer composite electrolyte films. Polym Eng Sci 2010;50(5):878–84.

[28] Sheha E. Preparation and physical properties of $(PVA)_{0.75}(NH_4Br)_{0.25}(H_2SO_4)_{xM}$ solid acid membrane. J Non-Cryst Solids 2010;356(43):2282–5.

[29] Bhargav PB, Mohan VM, Sharma AK, Rao VVRN. Structural and electrical studies of sodium iodide doped poly (vinyl alcohol) polymer electrolyte films for their application in electrochemical cells. Ionics 2007;13(1):173–8.

[30] Pradhan DK, Choudhary RNP, Samantaray BK. Studies of dielectric and electrical properties of plasticized polymer nano composite electrolytes. Mater Chem Phys 2009;115(2–3):557–61.

[31] Majid SR, Arof AK. Electrical behavior of proton-conducting chitosan-phosphoric acid-based electrolytes. Physica B 2007;390(1–2):209–15.

[32] Selvasekarapandian S, Baskaran R, Hema M. Complex AC impedance, transference number and vibrational spectroscopy studies of proton conducting PVAc–NH4SCN polymer electrolytes. Physica B 2005;357(3–4):412–9.

[33] Sheha E. Ionic conductivity and dielectric properties of plasticized $PVA_{0.7}(LiBr)_{0.3}(H_2SO_4)_{2.7M}$ solid acid membrane and its performance in a magnesium battery. Solid State Ionics 2009;180(36–39):1575–9.

[34] Prajapati GK, Roshan R, Gupta PN. Effect of plasticizeron ionic transport and dielectric properties of PVA–H_3PO_4 proton conducting polymeric electrolytes. J Phys Chem Solids 2010;71(12):1717–23.

[35] Reddy ChVS, Sharma AK, Rao VVRN. Electrical and optical properties of a polyblend electrolyte. Polymer 2006;47(4):1318–23.

[36] Jana S, Thapa R, Maity R, Chattopadhyay KK. Optical and dielectric properties of PVA capped nanocrystalline PbS thin films synthesized by chemical bath deposition. Phys E Low Dimens Syst Nanostruct 2008;40(10):3121–6.

[37] El-Khodary A. Evolution of the optical, magnetic and morphological properties of PVA films filled with $CuSO_4$. Physica B 2010;405(16):3401–8.

[38] Raja V, Sarma AK, Rao VVRN. Optical properties of pure and doped PMMA-CO-P4VPNO polymer films. Mater Lett 2003;57(30):4678–83.

[39] Mahendia S, Tomar AK, Kumar Sh. Nano-Ag doping induced changes in optical and electrical behaviour of PVA films. Mater Sci Eng B 2011;176(7):530–4.